Our conclusions are as follows:

For $J=1^-$ the required l mixing is such that the higher values are favored. It is expected that this is not the case.

For $J=2^\pm$ the smaller l values are favored. Thus, it is expected that the assignment of $J=2$ is best, however no assumption about the parity of the state may be made.

PHYSICAL REVIEW VOLUME 124, NUMBER 5 DECEMBER 1, 1961

Energy Levels of Na^{21} and Mg^{22}†

F. AJZENBERG-SELOVE
Haverford College, Haverford, Pennsylvania

AND

L. CRANBERG AND F. S. DIETRICH*
Los Alamos Scientific Laboratory, University of California, Los Alamos, New Mexico

(Received July 31, 1961)

Neon gas has been bombarded with 2.4, 3.1, 4.6, and 6.1-Mev deuterons and with 3.4- and 4.5-Mev He^3 particles. Time-of-flight measurements of neutron groups indicate excited states of Na^{21} at 0.37±0.04, 1.69±0.05, 2.83±0.04, 3.89±0.05, 4.86±0.06, and 5.01±0.05 Mev, in addition to the well-known states at 2.43, 3.57, 4.18, 4.31, and 4.49 Mev. Angular distributions show strong direct interaction features. Mg^{22}, here reported for the first time, has a mass excess $(M-A)$ of −0.14±0.08 Mev (C^{12} reference) from $Q=-0.043\pm0.08$ Mev for $Ne^{20}(He^3,n)Mg^{22}$. The first excited state is at 0.995±0.04 Mev. No other states are observed with $E_x<2.5$ Mev.

I. INTRODUCTION

In Ne^{21}, studies of the proton groups from the reactions $F^{19}(He^3,p)Ne^{21}$ (Hinds and Middleton[1]) and $Ne^{20}(d,p)Ne^{21}$ (Freeman[2]) have shown the existence of eleven states with excitation energies E_x less than 5 Mev. In the mirror nucleus Na^{21}, only eight states had been reported in the same energy interval when this work was begun. Thus this experiment was undertaken to locate the remaining states, to determine, if possible, their J^π, and to study the interaction mechanisms involved in the $Ne^{20}(d,n)Na^{21}$ reaction at deuteron energies at and above the Coulomb barrier.

The information[3] concerning the Na^{21} states come from two types of studies: the bound states have been observed in the $Ne^{20}(d,n)Na^{21}$ reaction, using plate,[4] spectrometer,[5] and counter-ratio[6] techniques; the unbound states have been determined by studying the interactions[7] of Ne^{20} and protons [$Ne^{20}(p,\gamma)Na^{21}$,[5,8,9] $Ne^{20}(p,p)Ne^{20}$,[10] and[11] $Ne^{20}(p,p')Ne^{20*}$]. The evidence for the observed states may be summarized as follows:

Ground state. The mass of Na^{21} is known[12] to 32 kev. The superallowed character of the β^+ decay to the ground state of Ne^{21} shows $J^\pi=\frac{3}{2}^+$.

0.37-Mev state. This state has been observed in $Ne^{20}(d,n)Na^{21}$. At $E_d=1$ Mev ($\theta=0°$ and 90°), Swann and Mandeville[4] reported a state with $Q=-0.17\pm0.05$ Mev which they tentatively assigned to the ground-state reaction. Angular distributions[5] at $E_d=2.7$, 4.5, and 4.9 show $l_p=2$ and therefore $J^\pi=(\frac{3}{2},\frac{5}{2})^+$ for this state.

1.73-Mev state. This state was previously reported to be located at 1.46±0.04 Mev by Marion, Slattery, and Chapman.[6] They used the counter ratio technique for locating the corresponding threshold in the (d,n) reaction. While we are in agreement with the other results reported by Marion *et al.* (see below), we disagree by over 200 kev with this determination. It may

† Work performed under the auspices of the U. S. Atomic Energy Commission and the National Science Foundation.

* Now at California Institute of Technology, Pasadena, California.

[1] S. Hinds and R. Middleton, Proc. Phys. Soc. (London) **74**, 779 (1959).

[2] J. M. Freeman, Phys. Rev. **120**, 1436 (1960).

[3] N. B. Gove, C. L. McGinnis, R. Nakasima, and K. Way, *Nuclear Level Schemes, Landolt-Börnstein Critical Tables* (Springer-Verlag, Berlin, 1961). We are indebted to Dr. F. Everling for this information concerning the $A=21$ and 22 level schemes.

[4] C. P. Swann and C. E. Mandeville, Phys. Rev. **87**, 215(A) (1952).

[5] R. E. Benenson and L. J. Lidofsky, Phys. Rev. **123**, 939 (1961).

[6] J. B. Marion, J. C. Slattery, and R. A. Chapman, Phys. Rev. **103**, 676 (1956).

[7] See P. M. Endt and C. M. Braams, Revs. Modern Phys. **29**, 68 (1957) for a review of the early work.

[8] N. W. Tanner, Phys. Rev. **114**, 1060 (1959); G. C. Thomas and N. W. Tanner, Proc. Phys. Soc. (London) **75**, 498 (1960).

[9] Valter, Gonchar, Lvov, and Tsytko, Iszv. Akad. Nauk SSSR, Ser. Fiz. **23**, 228 (1959).

[10] W. Haeberli, A. Galonsky, E. Goldberg, and R. Douglas, Phys. Rev. **91**, 438(A) (1953); W. Haeberli, *ibid.* **99**, 640(A) (1955).

[11] A. Galonsky, W. Haeberli, E. Goldberg, and R. Douglas, Phys. Rev. **91**, 439(A) (1953); M. C. Cox, J. J. van Loef, and D. A. Lind, *ibid.* **93**, 925(A) (1954).

[12] F. Everling, L. A. König, J. H. E. Mattauch, and A. H. Wapstra, Nuclear Phys. **18**, 529 (1960).

be that the location of a resonance in the total yield of neutrons, which occurs at about the same energy as the threshold, may somehow have affected the true position of the threshold. A state at 1.77±0.05 Mev has recently been reported.[5]

2.43-Mev *state.* The observation of this state has been reported by Marion *et al.*[6]; $Q=-2.201\pm0.007$ Mev. This is the Na^{21} state whose mass is known best. The (d,n) angular distributions indicate[5] $l_p=0$ and therefore $J^\pi=\frac{1}{2}^+$.

2.84-Mev *state.* Marion *et al.*[6] observed a threshold in $Ne(d,n)$ at $E_d=2.887\pm0.015$ Mev. Since an analogous level was not then known in Ne^{21}, they assigned the threshold to $Ne^{22}(d,n)Na^{23}$ ($E_x=9.01$ Mev in Na^{23}). If we assume the group to be due to the (d,n) reaction on Ne^{20}, $Q=-2.623\pm0.015$ Mev, $E_x=2.853\pm0.035$ Mev. This excitation energy is in good agreement with that of the Ne^{21} level at 2.87 Mev, and with the results which will be reported in Sec. III.

The states at 3.56, 4.18, 4.31, and 4.49 Mev. The first of these states has been seen in the $Ne^{20}(p,\gamma)Na^{21}$ reaction. The ground-state transition is very strong,[5,8] the level is formed by $l=2$ proton capture,[5] and the angular distribution of the 3.57-Mev γ rays[5,9] shows $J^\pi=\frac{3}{2}^+$ or $\frac{5}{2}^+$. The other states are observed[10,11] as resonances in (p,p) or (p,p') at $E_p=1.81$ ($\Gamma=180$ kev), 1.953 ($\Gamma=6$ kev), and 2.135 Mev ($\Gamma=17$ kev): $J^\pi=\frac{3}{2}^-$, $\frac{5}{2}^+$, and $\frac{3}{2}^+$, respectively. There is also observed an anomaly in the cross section at $E_p=2.7$ Mev. It is reported[10] that this anomaly cannot be analyzed in terms of a single state.

The existence of Mg^{22} has not been previously reported. Its mass may however be roughly calculated by assuming the charge independence of nuclear forces. The first state in the $T_z=0$ member of the $A=22$ triad, Na^{22}, which appears to be the $J^\pi=0^+$, $T=1$ analog of the ground states of Ne^{22} and of Mg^{22} is located[3] at 0.666 Mev. Since the mass excess $(M-A)$ of the Na^{22} ground state is -5.183 Mev,[12] the $(M-A)$ of the 0.666-Mev state is -4.517 Mev. The isobaric difference between Mg^{22} and Na^{22} is approximately 3.9 Mev [Coulomb energy difference, using $r_0=1.45$ fermis, less the $(n-H^1)$ mass difference] and therefore the $(M-A)$ of $Mg^{22}=-4.517+3.9$ Mev $=-0.6$ Mev. One can then calculate the Q of the $Ne^{20}(He^3,n)Mg^{22}$ reaction to be +0.4 Mev. While this calculation is admittedly crude, it is known[13] that in the light nuclei the agreement between analog states, when the adjustment is carried out in a similar way, is usually better than 0.4 Mev. And, in fact, when the mass of Ne^{22} is isobarically adjusted, the Ne^{22}-Na^{22} mass difference becomes +0.63 Mev, in excellent agreement with the position of the presumed $T=1$ state at 0.666 Mev.

One may expect the level structure in Mg^{22} to be similar to that of its mirror nucleus, Ne^{22}. The first three states of Ne^{22} are located at 0 ($J=0^+$), 1.274 ($J=2^+$), and 3.356 Mev ($J=1^-$, 2^+).

[13] F. Ajzenberg-Selove and T. Lauritsen, Ann. Rev. Nuclear Sci. **10**, 409 (1960).

II. EXPERIMENTAL PROCEDURES

The large Los Alamos vertical Van de Graaff generator was used to accelerate deuterons to energies of 2.5 to 6.2 Mev and He^3 particles to energies of 4.0 to 5.0 Mev. An rf electrostatic beam deflector, operated at a frequency of about 1.93 Mc/sec, is located in the high-voltage terminal of the accelerator. It serves to "chop" the charged particles into bursts and therefore permits use of time-of-flight measurements of neutrons emitted in nuclear reactions. After collimation in the beam tube, the incident particles encounter a gas target chamber.

The target consisted of a brass chamber insulated from the beam tube. The cylindrical chamber was 3 cm long and had a diameter of 0.9 cm. The front of the chamber was covered with 0.05-mil nickel foil. The back of the chamber was made of gold. Currents varied from 0.2 μamp to 1 μamp. Gases used were spectroscopically pure neon and tritium. The samples were subsequently assayed by Dr. T. Roberts.

The neutrons were detected by a proton recoil plastic scintillator coupled to a fast photomultiplier. The detector used in the (d,n) work was an NE 102 scintillator with $1\frac{3}{4}$-in. diameter and $1\frac{1}{2}$-in. length; that used in the (He^3,n) work was larger: 5 in. in diameter, $1\frac{1}{2}$ in. long. Both scintillators were canned with an aluminum reflector, surrounded by lead and placed inside large collimators.[14] The collimator used is set up on a rotatable mount so that it can be aimed at the target at any angle between 0° and ~160° with respect to the incident charged particle beam. The distance between the target and the detector was varied in this experiment up to a maximum of 4 m, the flight path being generally a compromise between resolution and available machine time.

The energy of the neutrons is determined by a measurement of the time required for the neutrons to travel the flight path between the target and the detector. This is accomplished by means of a time-to-pulse height converter and pulse-height analyzer. The details of the time measuring arrangement have been described previously.[15] The only change which has been made from the arrangement described in reference 15 is that the "stop" pulse is derived from a capacitative pickup cylinder, through which the pulsed beam passes, rather than from the deflecting voltage. This change became necessary when terminal pulsing was substituted for external pulsing of the beam.

[14] L. Cranberg and L. Rosen, *Nuclear Spectroscopy,* edited by F. Ajzenberg-Selove (Academic Press, Inc., New York, 1960), Vol. A, p. 411. The collimator enclosing the larger detector uses paraffin and lithium hydride as the moderating and capturing materials. It is 30 in. in outside diameter and about 48 in. long with a 5-in. diameter hole on the axis.

[15] W. Weber, C. W. Johnston, and L. Cranberg, Rev. Sci. Instr. **27**, 166 (1956).

The calibration of the output of the pulse-height analyzer in terms of time was determined in two ways: (1) For the $Ne^{20}(d,n)Na^{21}$ spectra, the time per channel was calculated on the basis of the de-excitation γ ray and the neutron group corresponding to the 2.431-Mev state; the Q value for that reaction is known to ± 7 kev. At each angle, and at each deuteron energy, the difference between the channel number corresponding to $t=0$ and the 2.43-Mev state neutron group was determined. The energy of the neutron group was calculated, and the corresponding flight time was obtained from the tables of Ribakov and Sidorov.[16] The flight time divided by the channel difference then gave t_c, the time per channel ($t_c \simeq 2.28$ nsec/channel). (2) In the case of the $Ne^{20}(He^3,n)Mg^{22}$ reaction no known group could be used for calibration. Instead, tritium gas was bombarded by 2.50-Mev protons and the neutrons emitted at 0° from the $T(p,n)He^3$ reaction, whose energy could be calculated accurately, were detected at various flight paths ranging from 1.0 to 3.0 m. This flight path variation not only led to determinations of t_c but also showed the linearity of the time versus channel plot. Unfortunately, no t_c calibration was made on the day on which the best (He^3,n) runs were made, but calibrations taken the days preceding and following that day indicate $t_c=2.32$ nsec/channel.

In both cases the uncertainties in the t_c determinations are, of course, included in the quoted uncertainties of the Q values we obtained.

The detector sensitivity had been determined previously[17] by observing the known 0° yield of the $T(p,n)He^3$ and $D(d,n)He^3$ reactions as a function of neutron energy. The over-all gain and effective bias of the detection system were adjusted daily on the basis of pulses produced by the 60-kev γ ray from an americium-241 source, thereby duplicating the conditions under which the detector sensitivity had been determined. Americium-241 produces a characteristic peak at about the same pulse heights as do neutrons of energies near the cut-off region of the detector sensitivity curve,[17] so that gain and discriminator settings may be made in terms of the 60-kev γ rays, thereby compensating for drifts of the electronic system. The absolute sensitivity may be calculated in terms of the known cross section of the $T(p,n)He^3$ reaction. This calculation will be discussed further in Sec. III.

Finally, the question of background must be considered. All runs were immediately preceded or followed by a background run in which the gas chamber was evacuated. The background showed some structure, primarily due to the $C^{12}(d,n)N^{13}$ reaction. The carbon was probably in the form of a deposit on the nickel foil at the chamber entrance. Generally background runs were shorter than the foreground runs. The IBM-704 computer at Los Alamos, which processed the raw data, subtracted the background runs, suitably corrected for any difference in incident beam charge, from the foreground runs. Longer runs were desirable in the backward direction because the neutron angular distributions were peaked in the forward direction. However, for ease in computing angular distributions, the 704 was programmed to normalize the "true" data (foreground less background) at all angles and energies to the same incident beam charge (approximately 107 μcoul per run) and to the same target thickness (the pressure of the gas varied slightly from one run to another).

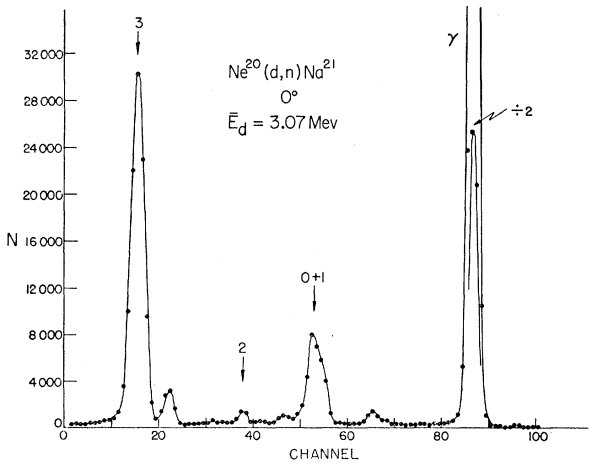

FIG. 1. The time spectrum of neutrons from the $Ne^{20}(d,n)Na^{21}$ reaction for an incident energy of 3.07 Mev, as seen at 0° to the deuteron direction. The numbered peaks correspond to states in Na^{21} as indicated in Fig. 18. When sample statistical errors are not indicated, the error is contained within the data point. The flight path was 2.02 m.

[16] B. V. Ribakov and V. A. Sidorov, Suppl. Atomnaya Energ. 6, (1958).

[17] D. M. Thomson, Ph.D. thesis, University of Kansas, 1960 (unpublished); available from University Microfilms, Ann Arbor, Michigan.

III. Na^{21} RESULTS

The $Ne^{20}(d,n)Na^{21}$ reaction was studied at $\bar{E}_d=2.37$, 3.07, 4.60, and 6.12 Mev. The $\bar{E}_d=2.37$ Mev run was

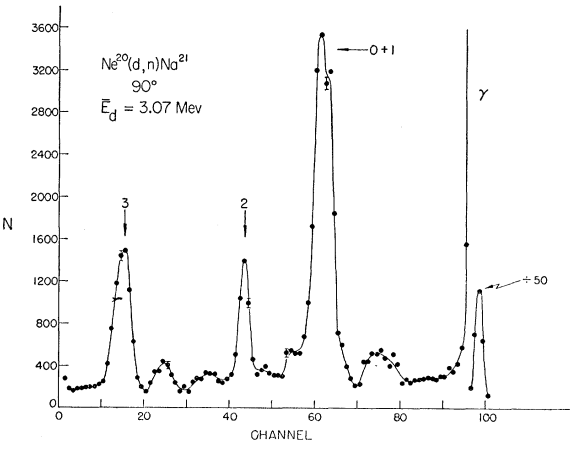

FIG. 2. The data at 90°, $\bar{E}_d=3.07$ Mev (see also caption of Fig. 1).

made at only one angle, 0°, and with good resolution to resolve the ground and first excited states of Na^{21}. The runs at the higher energies were concerned with the higher excited states and with the interaction mechanisms; they were carried out at 11 angles ranging from 0° to 150° in the laboratory system.

A. 3.07-Mev Run

The incident energy of the deuteron beam was 3.20 Mev. The 0.05-mil Ni window corresponded to an energy loss of 0.11 Mev. The pressure of the neon gas was 100 mm of Hg, and thus the average energy of the deuterons in the target was 3.07 Mev. Typical spectra are shown in Figs. 1 and 2. No attempt was made to separate the ground and first excited states (groups 0+1) but indication of structure is evident. The 1.73- and 2.43-Mev groups appear clearly (groups 2 and 3, respectively). Relative to the 2.43-Mev state (see Sec. II), the Q value of group 2 is determined to be -1.46 ± 0.01 Mev. [The error quoted here is the standard deviation of the results from seven angles; in the backward direction, the groups due to the 2.43-Mev state were not clearly enough observed to be used as references.]

The neon gas used was an isotopic sample: it contained 8.85% of the Ne^{22} isotope.[18] The $Ne^{22}(d,n)Na^{23}$ reaction accounts for the subsidiary structure seen in Figs. 1 and 2. For instance, at 0° and at 90°, the groups centered at channels 22 and 25 are due to an excited state of Na^{23} at 8.41 ± 0.03 Mev. [The shift to higher channel from 0° to 90° may seem surprising, but it should be noted that the γ-ray peak is shifted also. This was done deliberately to obtain a more convenient display.] It is clear that these groups are due to an excited state in Na^{23} because a few runs were made with isotopically pure[19] Ne^{22} and these groups were strongly

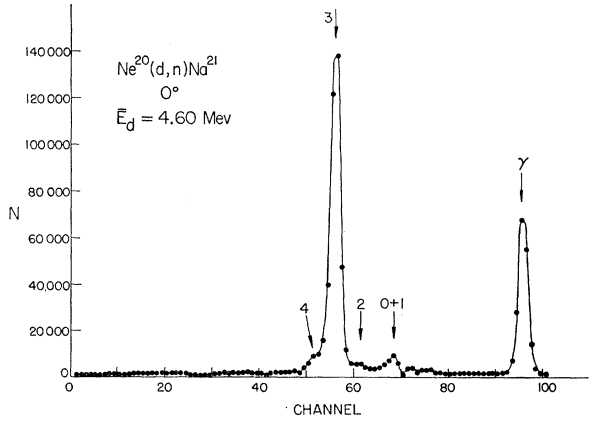

FIG. 3. The data at 0°, $\bar{E}_d = 4.60$ Mev (see also caption of Fig. 1).

[18] The neon was assayed by Dr. T. Roberts to whom we are indebted for the following information: Ne^{20}, 90.89%, Ne^{21}, 0.260%, Ne^{22}, 8.85%, traces of N and O.

[19] We are grateful to Dr. N. Jarmie and Dr. M. G. Silbert who made the Ne^{22} available to us.

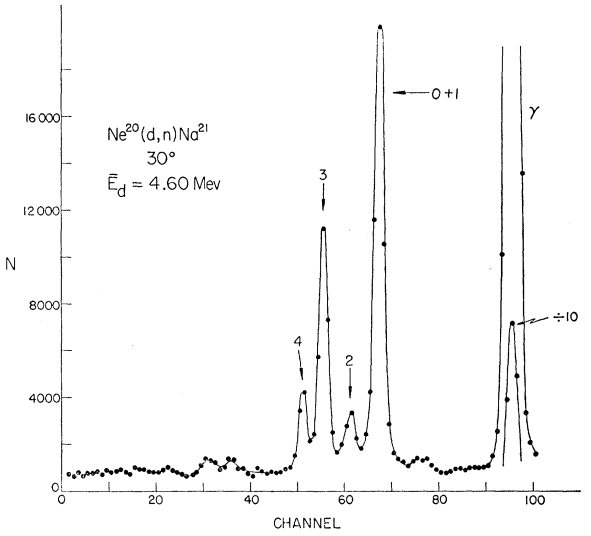

FIG. 4. The data at 30°, $\bar{E}_d = 4.60$ Mev (see also caption of Fig. 1).

evident. Marion *et al.*[6] had observed a threshold in the (d,n) reaction on neon at $E_d = 2.292 \pm 0.010$ Mev. Since no analogous state is known[1,2] in Ne^{21}, the authors suggested that the threshold was connected with the $Ne^{22}(d,n)Na^{23}$ reaction: $E_x = 8.431 \pm 0.011$, in excellent agreement with our result. Finally, the high-energy structure in the 90° data (Fig. 2) can also be accounted for by the Ne^{22} contribution.

B. 4.60-Mev Run

The incident energy of the deuteron beam was 4.70 Mev. The 0.05-mil Ni window corresponded to an energy loss of 0.08 Mev. The pressure of the neon gas was 100 mm of Hg and therefore $\bar{E}_d = 4.60$ Mev. Typical spectra are shown in Figs. 3–5. The weighted Q value from the runs at 4.60 Mev, corresponding to neutron groups "2" is -1.49 ± 0.04 Mev, in excellent agreement

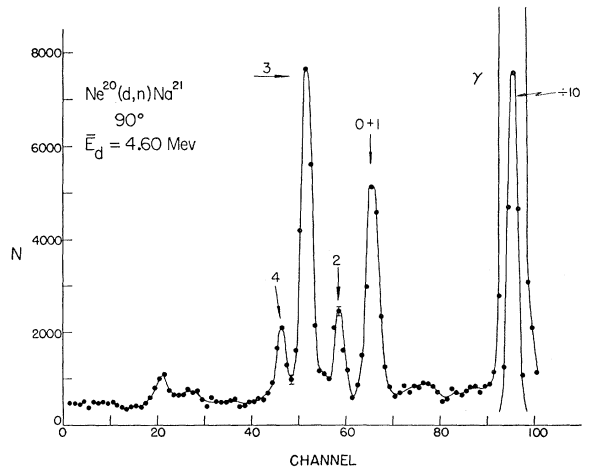

FIG. 5. The data at 90°, $\bar{E}_d = 4.60$ Mev (see also caption of Fig. 1).

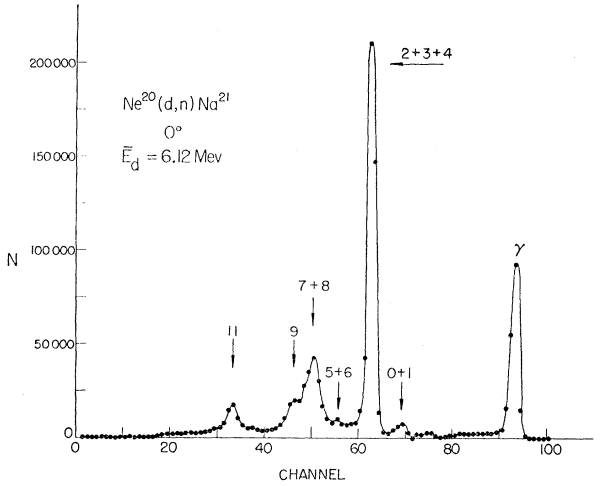

FIG. 6. The data at 0°, $\bar{E}_d$=6.12 Mev (see also caption of Fig. 1).

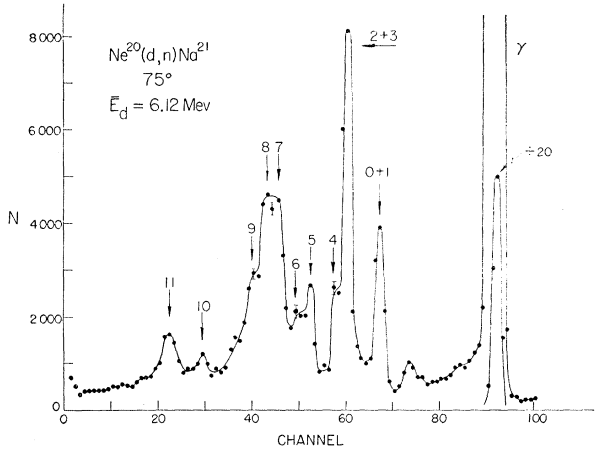

FIG. 8. The data at 75°, $\bar{E}_d$=6.12 Mev (see also caption of Fig. 1).

with the E_d=3.07 Mev results and in disagreement with the results of Marion *et al.* (see Sec. I). At all angles except 0° and 15° there also appear resolved neutron groups corresponding to an excited state of Na^{21} at 2.83±0.04 Mev (groups labeled "4"). [See the introduction for a discussion of Marion's results[6] relating to this level.]

C. 6.12-Mev Run

The incident energy of the deuteron beam was 6.21 Mev. The loss in the Ni window was 0.07 Mev. The pressure of neon was 100 mm of Hg. Therefore $\bar{E}_d$=6.12 Mev. Typical spectra are shown in Figs. 6–10. In addition to the groups (not always resolved) corresponding to the first five states of Na^{21}, six other groups appear.

(1) Groups labeled "5": These appear most clearly at 75°, 90°, and 105°. The groups correspond to the $J=\frac{5}{2}^+$ level at 3.57 Mev observed in $Ne^{20}(p,\gamma)Na^{21}$.

(2) Groups labeled "6": Based on the 90° and 105° data, $Q=-3.66\pm0.04$ Mev, $E_x=3.89\pm0.05$ Mev. This state has not been observed in the $(Ne^{20}+p)$ work.

Since the $Ne^{20}(p,p)$ work[10] has not been published, it is not known whether a resonance (at $E_p\sim1.5$ Mev) corresponding to such a state is definitely excluded. Of course it is not completely excluded that the groups "6" are due to $Ne^{22}(d,n)Na^{23}$. However the groups are relatively intense and the mirror region shows three states (of unknown J^π) with E_x=3.67, 3.74, and 3.89 Mev.

(3) Groups labeled "7" and "8": These groups, corresponding to the 4.18- and 4.31-Mev states are never fully resolved, although the 90° and 105° spectra suggest the presence of two separate groups. The intensities of the groups do not differ greatly. From an analysis[10] of the $(Ne^{20}+p)$ resonances, $J=\frac{3}{2}^-$ and $\frac{5}{2}^+$. The l_p should then be 1 and 2, respectively.

(4) Groups labeled "9": These groups are indicated at all angles but are never fully resolved. They correspond to the $J=\frac{3}{2}^+$ state at 4.49 Mev observed in $(Ne^{20}+p)$.

(5) Group labeled "10": This group appears clearly only at 75°. If it belongs to $Ne^{20}(d,n)Na^{21}$, $Q=-4.63\pm0.05$, $E_x=4.86\pm0.06$ Mev. It is not excluded that Ne^{22} is involved. The intensity argument cannot be made here. One can only say that additional states in

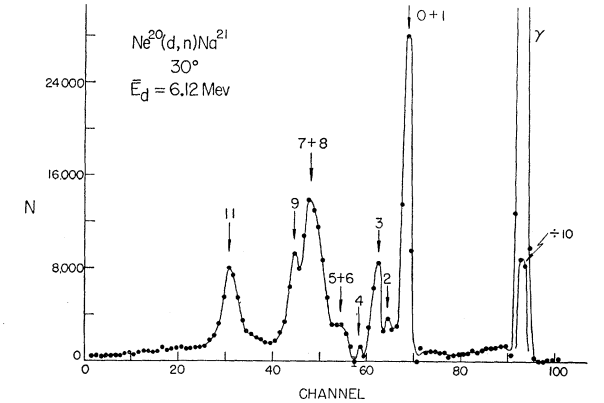

FIG. 7. The data at 30°, $\bar{E}_d$=6.12 Mev (see also caption of Fig. 1).

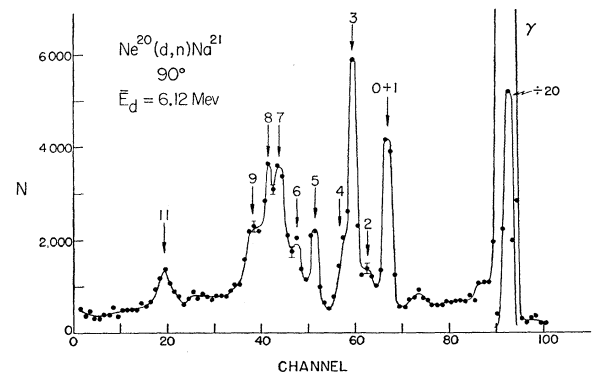

FIG. 9. The data at 90°, $\bar{E}_d$=6.12 Mev (see also caption of Fig. 1).

Na^{21} are needed in this energy region because of the Ne^{21} structure. Haeberli[10] does not report a resonance at 2.52 Mev corresponding to this state. However, attempts to analyze the 2.7-Mev resonance (see below) in terms of a single state have not been successful. It may be that the 4.86-Mev state is involved. The J value of this state is probably high since the intensity is relatively low.

(6) Groups labeled "11": These groups are clearly resolved at all angles: $Q=-4.78\pm0.03$ Mev, $E_x=5.01\pm0.05$ Mev. Presumably this state is involved in the 2.7-Mev complex resonance observed[10] by Haeberli in $(Ne^{20}+p)$.

D. 2.37-Mev Run

The incident energy of the deuteron beam was 2.51 Mev. The loss in the Ni foil was 0.13 Mev. The target was thin: 28 mm of Hg pressure of neon. The average deuteron energy was therefore 2.37 Mev. Data were taken at 0° only. The spectrum is shown as Fig. 11. It shows two resolved neutron groups corresponding to the ground state of Na^{21} and to a state at 0.37 ± 0.04 Mev. The intensities of the two groups are nearly the same.

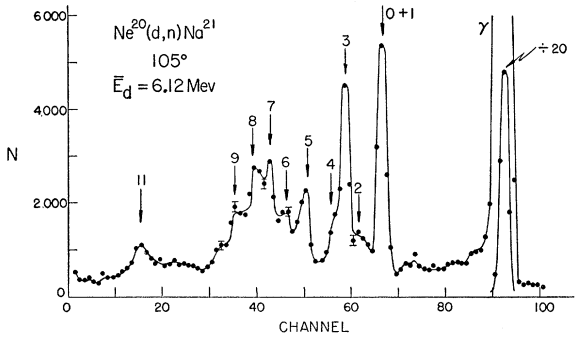

FIG. 10. The data at 105°, $\bar{E}_d=6.12$ Mev (see also caption of Fig. 1).

E. Cross Sections

The observed angular distributions are displayed in Figs. 12 to 17. The ordinates show the relative cross sections in the c.m. system in units which are arbitrary but which are the same in all the figures. The differential cross sections in millibarns per steradian, at the peak of the angular distributions of each of the neutron groups, are shown in Table I. While the relative cross sections are accurately determined, the absolute cross sections are only known to within about 30%. This figure includes an uncertainty of 20% in the counter efficiency and of 10% in the number of target nuclei. Table I also includes values of the reduced widths.

F. Angular Distributions

The angular distributions of the neutron groups were analyzed in terms of the Butler-Born theory, using the Lubitz[20] tables, and in terms of the distorted wave Born approximation (DWBA) method used by Tobocman.[21] While the gross structure of the distributions was usually well matched by the Butler-Born theory using a 5-fermi radius parameter, there was better over-all agreement with the DWBA curves.

These curves were obtained by using a program prepared by W. Tobocman and W. Gibbs and described

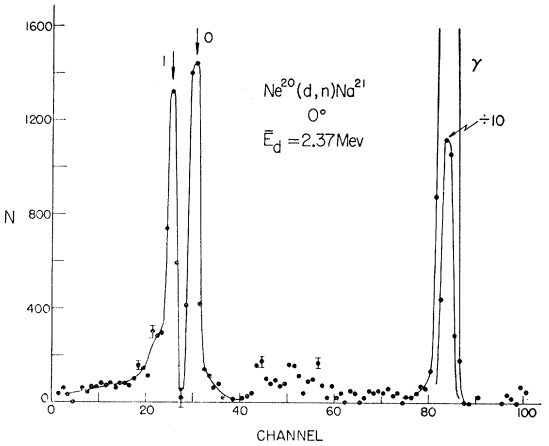

FIG. 11. The data at 0°, $\bar{E}_d=2.37$ Mev. The group marked 0 corresponds to the ground state of Na^{21}, that marked 1 to the first excited state of Na^{21} at 0.37 ± 0.04 Mev. The flight path was 3.02 m.

TABLE I. Differential cross sections[a] at peak[b] of angular distributions.

Excitation energies (Mev)[c]	Cross sections in mb/sr at $\bar{E}_d=3.07$ Mev		$\bar{E}_d=4.60$ Mev		$\bar{E}_d=6.12$ Mev		Reduced widths[e] $(2J+1)\theta^2$	
0 0.37	11.8	(48°)	12.5	(42°)	16.9	(32°)	0.12[f]	(2)
1.73	0.9	(97°)	1.6	(38°)	[d]		0.2[g,h]	(4)
2.43	34	(0°)	77	(0°)	119	(0°)	0.77[f,i]	(0)
2.84	...		4.0	(0°)	...		0.04[g]	(0)
4.18 4.31	...		...		31	(0°)	0.18[f]	(1)
4.49	...		...		13.6	(0°)	0.11[f]	(1)
5.01	...		...		13.6	(0°)	0.25[f]	(1)

[a] The estimated uncertainty in these cross sections is ±30%: see Sec. III-E.
[b] The peak angle in the c.m. system is indicated in parentheses to the right of the cross-section value.
[c] States in brackets were not resolved: the cross section is that of the composite group.
[d] The total cross section for formation of this state is less than at $\bar{E}_d=4.60$ Mev.
[e] These reduced widths have been calculated from formula II.29 of the article by M. H. MacFarlane and J. B. French [Revs. Modern Phys. **32**, 567 (1960)] using $r_0=5$ fermi and $\sigma_{TAB}{}^l$ taken from reference 20. The assumed l_p are indicated in parentheses.
[f] This value is derived from the 6.12-Mev cross section.
[g] This value is derived from the 4.60-Mev cross section.
[h] This reduced width was obtained by "fitting" the theoretical curve at 95°, even though the fit is extremely poor.
[i] Because the energy of this state is so nearly the proton separation energy, formula II.40 of MacFarlane and French was used in determining this reduced width.

[20] C. R. Lubitz, University of Michigan Report, 1957 (unpublished).
[21] W. Tobocman, Phys. Rev. **115**, 98 (1959).

in a report by Rodberg.[22] The calculations were carried out by Swartz[23] at the Los Alamos IBM-704 (Code STR). The parameters used in calculating the curves were:

R_N, radius of captured nucleon shell-model potential $=3.8$ f;
R, cutoff radius$=7$ f;
V_d, depth of real potential for deuteron-target nucleus interaction$=-50$ Mev;
W_d, depth of imaginary potential$=-30$ Mev;
a_d, diffuseness parameter$=0.8$ f;
$R_d=3.4$ f;
V_p, depth of real potential for neutron-residual nucleus interaction$=-50$ Mev;
W_p, depth of imaginary potential$=-8$ Mev;
a_p, diffuseness parameter$=0.5$ f;
$R_p=2.9$ f.

Of course E_d, Q, and l_p (the orbital angular momentum of the captured proton) varied from case to case. ϵ_d, the deuteron binding energy, had to be artificially raised above 2.225 Mev in all but two cases in order to keep the calculation from blowing up. The sum of ϵ_d and Q must be greater than about 0.2 Mev. The variation in ϵ_d does not affect the shape of the distribution but it does affect the absolute differential cross sections[22] $[\sigma(\theta)\sim\sqrt{\epsilon_d}]$.

These parameters, suggested by Rodberg, led to angular distributions which fitted the set of experimental curves overall well in shape but poorly in absolute cross sections. In one case, that for $Q=0$, $\bar{E}_d=4.60$ Mev (see below), a number of the parameters were varied to observe their contribution. The cross section, for instance, is strongly dependent on R_N: an increase of a little over 10% in R_N led to a doubling of the peak cross section. No attempt was made to fit the absolute magnitudes of the cross sections because there did not seem to be a consistent dependence between the theoretically predicted cross sections and the experimentally observed ones (see the discussion which follows).

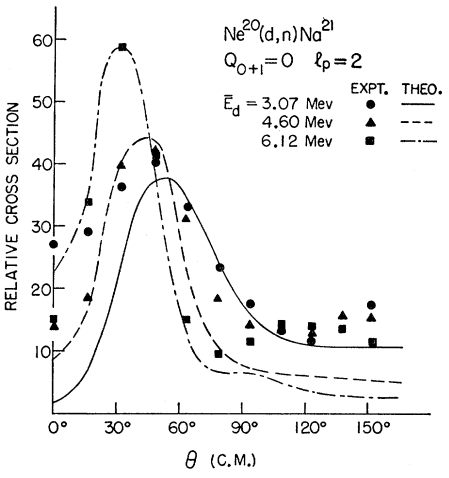

FIG. 12. Angular distributions in the center-of-mass system for the neutrons (unresolved) to the ground and first excited states of Na^{21} at $\bar{E}_d=3.07$, 4.60, and 6.12 Mev. When statistical errors are not indicated, they are contained within the data points. The relative intensities are arbitrary, but the units used are the same in Figs. 12–18. The curves are calculated from the distorted-wave Born approximation theory (see Sec. III-F for details).

[22] L. S. Rodberg, Los Alamos Scientific Laboratory Report, 1960 (unpublished).

[23] We are very indebted to Mr. Blair Swartz for his kindness in arranging these calculations.

*Ground+0.37-*Mev *states* (*Fig. 12*). The two unresolved groups were plotted as an entity with $Q_{0+1}=0$ Mev. The states are believed to be $\frac{3}{2}^+$ and $\frac{5}{2}^+$ and the l_p should therefore be 2. The data obtained at $\bar{E}_d=3.07$, 4.60, and 6.12 Mev may be compared with the theoretical curves. The magnitudes of the peaks of the theoretical curves were, in each case, arbitrarily fitted to the peaks of the smooth curves (not shown on the figure) drawn through the data points. The agreement of the shapes in the $\bar{E}_d=4.60$- and 6.12-Mev cases is good except in the backward direction where the theoretical curves are, typically, too low. The $\bar{E}_d=3.07$ Mev curve poorly reproduces the data points at forward angles. The theoretical cross sections were calculated using a "J"$=\frac{9}{2}$ for the group $[\sigma(\theta)\sim 2J+1]$ to compensate for the presence of the two states ($2J_0+1=4$, $2J_1+1=6$; therefore 2 "J"$+1=10$). The ratios of the theoretical and the experimental peak cross sections (for the latter, see Table I) are 0.41 (3.07 Mev), 0.50 (4.60 Mev), and 0.45 (6.12 Mev).

*1.73-*Mev *state* (*Fig. 13*). It is suggested by Benenson and Lidofsky,[5] on the basis of a collective model[24] calculation, that this state, with $Q=-1.50$ Mev, has $J=\frac{7}{2}^+$, which would involve $l_p=4$. The DWBA calcula-

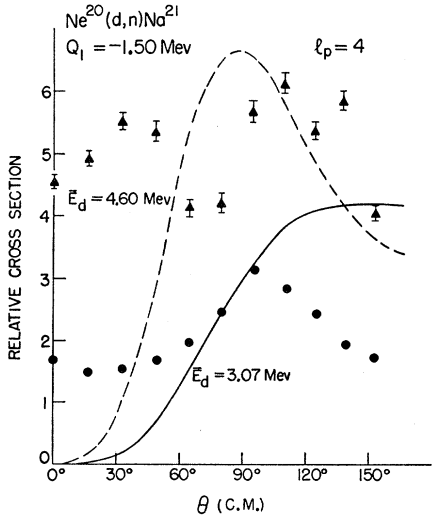

FIG. 13. Angular distributions in the c.m. system for the neutrons to the 1.73-Mev state of Na^{21} ($\bar{E}_d=3.07$ and 4.60 Mev). (See also caption of Fig. 12.)

[24] G. Rakavy, Nuclear Phys. 4, 375 (1957).

tions for this case are shown in Fig. 13 (plotted in arbitrary units but in proper relation for the two energy cases) even though they bear little resemblance to the experimental data. This is the only state for which the DWBA approach, and the Butler-Born approach, do not seem to be applicable. Assuming $J=\frac{7}{2}^+$, $l_p=4$, the ratio of the theoretical and experimental cross sections are 0.074 (3.07 Mev, 97°), 0.064 (4.60 Mev, 110°).

2.43-Mev *state* (*Fig. 14*). This state ($Q=-2.20$ Mev) is known to have $J=\frac{1}{2}^+$: $l_p=0$. The fit of the DWBA curves is good. One may notice that the experimental rise near $\theta=50°$ ($\bar{E}_d=6.12$ Mev) is also indicated in the calculated curve. The theoretical curves were separately normalized to each of the 0° data points. The cross-section ratios at 0° are 0.94, 0.80, and 0.47 for $\bar{E}_d=3.07$, 4.60, and 6.12 Mev. The ϵ_d used to obtain these ratios was 2.225 Mev; that used in the theoretical calculations was 2.7 Mev.

2.84-Mev *state* (*Fig. 15*). The J^π assignment for this state, with $Q=-2.61$ Mev, is not known. DWBA curves for $l_p=0$ and 1 ($\bar{E}_d=4.60$ Mev) are indicated on the figure. The fit of the forward angles with $l_p=0$ is good in shape if not in cross section. At 0°, the cross-section ratio (taking into account $\epsilon_d=3.2$ Mev) is 8.7 ($l_p=0$, J assumed to be $\frac{1}{2}$), 10.8 ($l_p=1$, J taken to be $\frac{5}{2}$). The curve for $l_p=2$ does not peak in the forward direction.

4.18 and 4.31-Mev *states* (*Fig. 16*). These states were not resolved and the angular distribution is a composite one. The J^π have been given[10,11] as $\frac{3}{2}^-$, $\frac{5}{2}^+$. The distribution should then be $l_p=1$ and 2 combined. The $l_p=1$ DWBA curve was normalized to the 0° point; the $l_p=2$ curve is then plotted to scale. The agreement

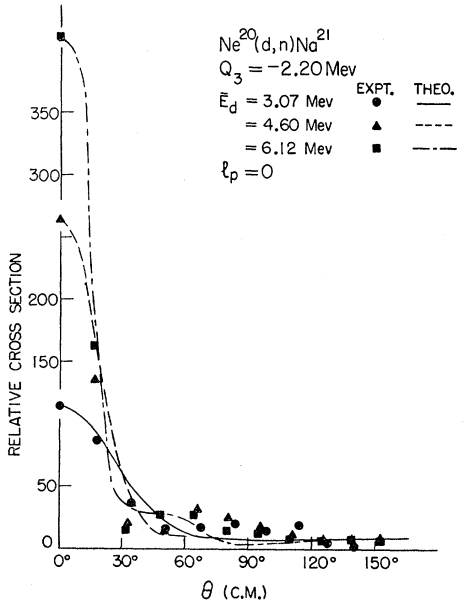

FIG. 14. Angular distributions in the c.m. system for the neutrons to the 2.43-Mev state of Na^{21} ($\bar{E}_d=3.07$, 4.60, and 6.12 Mev). (See also caption of Fig. 12.)

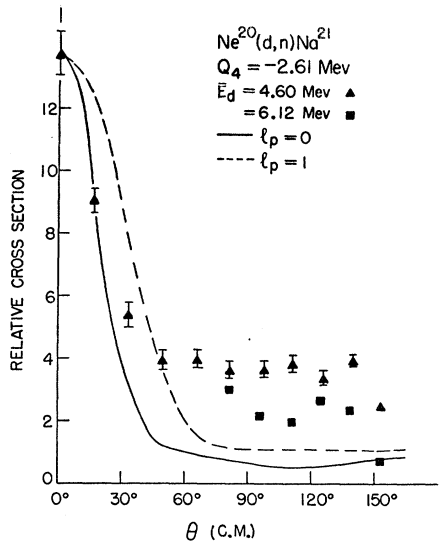

FIG. 15. Angular distributions in the c.m. system for the neutrons to the 2.84-Mev state of Na^{21} ($\bar{E}_d=4.60$ and 6.12 Mev). (See also caption of Fig. 12.)

is good if one bears in mind the composite nature of these data. Assuming that about 80%[25] of the experimental cross section (at 0°) is due to the $J=\frac{3}{2}^-$ state ($l_p=1$) and taking into consideration the value used for ϵ_d (4.6 Mev), the cross-section ratio is 0.5.

4.49 and 5.01-Mev *states* (*Fig. 17*). These states with $Q=-4.26$ and -4.78 Mev were resolved. The data points are however compared with the same theoretical curves since the curves are nearly the same (the Q dependence on E_d is not very strong) and the data points are very similar. It should be pointed out that the experimental points are plotted in the same arbitrary units and that, in fact, the differential cross sections for the two levels are identical at 0° (see Table I).

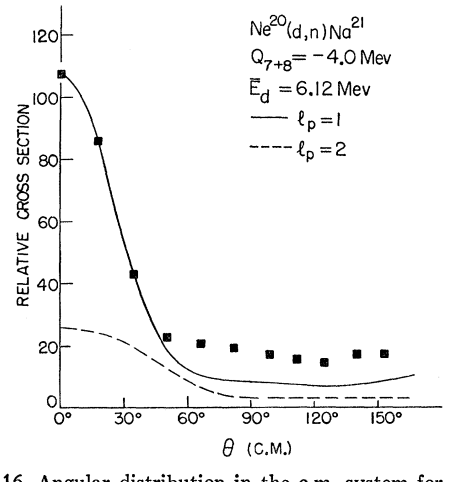

FIG. 16. Angular distribution in the c.m. system for the neutrons (unresolved) to the states of Na^{21} at 4.18 and 4.31 Mev ($\bar{E}_d=6.12$ Mev). (See also caption of Fig. 12.)

[25] From the ratio of the theoretical curves for $l_p=1$ and 2.

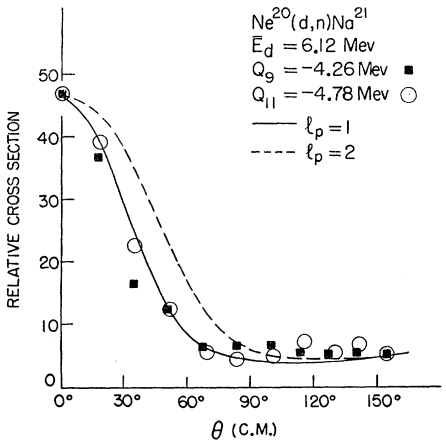

FIG. 17. Angular distribution in the c.m. system for the neutrons to the 4.49-Mev and 5.01-Mev states of Na^{21} (E_d=6.12 Mev). (See also caption of Fig. 12.)

The two theoretical curves were separately normalized to the 0° points. The agreement with the $l_p=1$ curve is excellent, although $l_p=2$ (with different values of some of the parameters) is not excluded. The $Q=-4.26$ Mev state has been said[10,11] to be $J=\frac{3}{2}^+$, which would imply $l_p=2$. Since the data relating to this value have not been published, it may be that $J=\frac{3}{2}^-$, and hence $l_p=1$, is a possibility. In any case, the similarities in shape and absolute cross sections argue that the l_p involved in the formation of both states are the same. Assuming $l_p=1$, $J=\frac{3}{2}$, the cross-section ratio for either state is 0.29 (corrected for $\epsilon_d=5.5$ Mev); for $l_p=2$, $J=\frac{3}{2}$, it is 0.095.

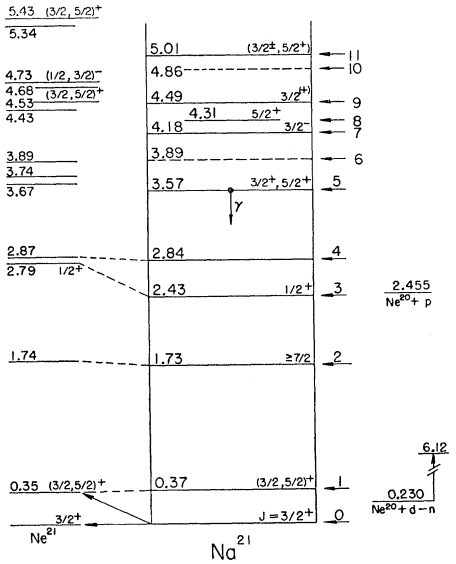

FIG. 18. Energy level diagrams of the mirror nuclei Ne^{21} and Na^{21}. The values for E_x (in Mev) and J^π are derived primarily from the summary of K. Way and her group [Landolt-Börnstein, *Nuclear Energy Levels*, Springer-Verlag, Berlin, Germany, 1961] and from the results presented in this paper. The ground states of Ne^{21} and Na^{21} have been arbitrarily adjusted to show the similarities in the level structure. Mirror states are connected by dashed lines. All levels shown in Ne^{21} are bound. The numbers (0 to 11) to the right of the Na^{21} diagram identify the corresponding neutron groups.

In summary then, the cross section ratios (theoretical to experimental) are in the range 0.3 to 1.0, for the most probable l_p values, except in two cases: those of the states at 1.73- and 2.84-Mev excitation energy.

The summary of these and other results on the levels of Na^{21} are shown in Table II and in Fig. 18.

IV. EXPERIMENTAL RESULTS: Mg^{22}

Only two successful runs were made on the $Ne^{20}(He^3,n)Mg^{22}$ reaction because of time limitation and the very low cross section of the reaction. The successful runs were made with He^3 particles[26] accelerated to 3.99 Mev and with the detector positioned at 0° and 60° with respect to the incident beam: see Figs. 19 and 20. Because of the low yield of neutrons, the large 5 in.×1.5 in. counter was used. The target chamber was operated at a pressure of 70 mm of Hg, corresponding to an energy loss[27] of about 150 kev in the neon gas. The 0.05-mil nickel foil at the entrance to the chamber degraded the energy of the He^3 beam by 0.5 Mev. Thus the average incident energy of the He^3 particles was 3.40 Mev with an uncertainty of about 0.05 Mev due principally to uncertainty in the energy loss in the nickel.

Two groups are observed at 0° and 60°; the group labeled 0 is presumably due to the ground state of Mg^{22}, that labeled 1 to the first excited state. No other groups are observed corresponding to states with $E_x<2.5$ Mev. Both of the observed states are bound and the origin of the relatively high plateau is not known (the spectra are "true," that is the background has been subtracted).

There is excellent agreement of the results from the 0° and 60° runs: $Q_0=-0.04(2)$ (0°), $-0.04(5)$ Mev

TABLE II. Energy levels of Na^{21}.

Level number	$Ne^{20}(d,n)Na^{21}$: Q in Mev (previous work)[a]	(this work)	'Best' E_x (in Mev)	J^π
0	+0.230±0.030[b]	[c]	0	$\frac{3}{2}^+$
1	−0.10 ±0.03	−0.14±0.04	0.37 ±0.04	$(\frac{3}{2},\frac{5}{2})^+$
2	−1.24 ±0.02 / −1.55 ±0.05 [d]	−1.46±0.04	1.73 ±0.04	$\geqslant\frac{7}{2}$
3	−2.201±0.007	−2.201[e]	2.431±0.031	$\frac{1}{2}^+$
4	−2.58 ±0.06	−2.60±0.02	2.84 ±0.04	
5	−3.343±0.035[f,g]	[c]	3.573±0.035	$\frac{3}{2}^+,\frac{5}{2}^+$
6		−3.66±0.04	3.89 ±0.05	
7	−3.95 ±0.05[f,g]	[c]	4.18 ±0.05	$\frac{3}{2}^-$
8	−4.084±0.035[f,g]	[c]	4.314±0.035	$\frac{5}{2}^+$
9	−4.258±0.035[f,g]	[c]	4.488±0.035	$\frac{3}{2}(^+)$
10		−4.63±0.05	4.86 ±0.06	
11	−4.8[d,g]	−4.78±0.03	5.01 ±0.05	$(\frac{3}{2}^\pm,\frac{1}{2}^-,\frac{5}{2}^+)$

[a] For references, see discussion in Sec. I.
[b] Calculated from masses given in reference 12.
[c] Group observed but no attempt made to obtain accurate Q value.
[d] See discussion in text.
[e] This group used as standard to determine all the other Q values listed in this column.
[f] Estimated error since error in resonance energy is not stated in original reference.
[g] These levels were observed in the interaction of protons with Ne^{20}. The listed Q values for the $Ne^{20}(d,n)Na^{21}$ reaction were calculated on the basis of the proton resonance energies and the binding energy of a proton in Na^{21}.

[26] We are indebted to Dr. H. E. Wegner who made the He^3 gas available to us.
[27] W. Whaling, *Handbuch der Physik* (Springer-Verlag, Berlin, 1958), Vol. 34.

(60°); $Q_1=-1.03(7)$ (0°), $-1.03(9)$ Mev (60°). And while the absolute accuracy of the Q values is not very high because of the uncertainty in the incident He^3 energy, the excitation energy of the excited state is well determined: $E_x=0.995\pm0.04$ Mev (the error given arises from the uncertainty in the t_c value). This excitation energy is consistent with the energy (1.274 Mev) of the first excited state in Ne^{22}. The Q_0 and Q_1 values are estimated to be -0.04 ± 0.08 and -1.04 ± 0.08 Mev. The Q_0 value leads to a mass excess $(M-A)$ for $Mg^{22}=-0.14\pm0.08$ Mev (based on C^{12}, and on the Mattauch-Wapstra masses[12] for Ne^{20}, He^3, and n). The lowest particle binding energy in Mg^{22} is then 5.22 Mev for $(Na^{21}+p)$.

The relative yields of the 0 and 1 groups are consistent with their presumably $J=0^+$ and 2^+ character. Group 1 should become relatively stronger at 60°. An extremely rough calculation of the differential cross section at 0° of the ground-state group suggests 0.5 mb/sr. This is a reasonable value for a (He^3,n) group.[28]

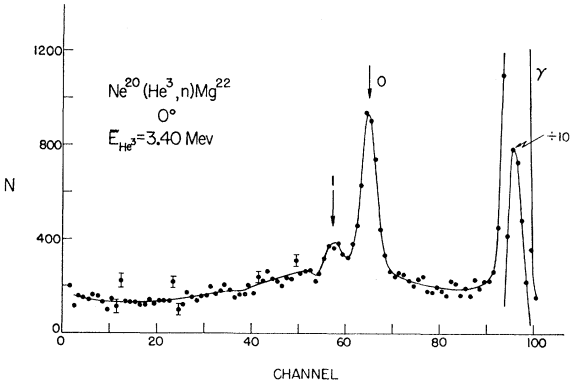

FIG. 19. The time spectrum of neutrons from the $Ne^{20}(He^3,n)Mg^{22}$ reaction for an incident energy of 3.40 Mev, as seen at 0° to the incident He^3 beam. The peak labeled 0 corresponds to the ground state of Mg^{22}, that labeled 1 to the state at 0.995 Mev. The flight path was 1.97 m.

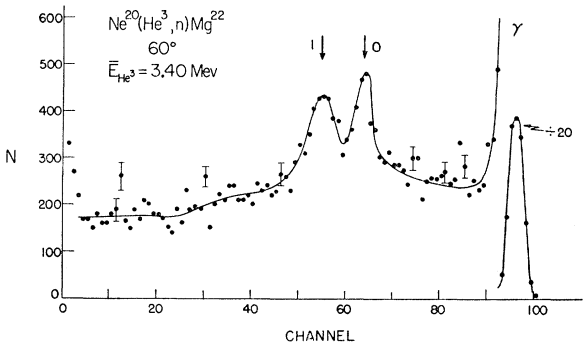

FIG. 20. The data at 60°, $\bar{E}(He^3)=3.40$ Mev (see also caption of Fig. 19).

This experiment is obviously a very preliminary one. One of us (F.A.S.) plans to repeat it in the near future. It is reported here only because of the complete lack of experimental information on Mg^{22}.

ACKNOWLEDGMENTS

We are very grateful to the staff of the P-9 group, and in particular to Dr. J. S. Levin and to Mrs. Dana Douglass, for their valuable assistance. We are much indebted also to Dr. J. L. McKibben for the design and construction of the terminal pulser used in this work. It is a pleasure to thank Dr. L. S. Rodberg and Professor W. Selove for their very helpful comments on the analysis of the data. One of us (F.A.S.) wishes to express her deep appreciation to the Los Alamos Scientific Laboratory for a thoroughly enjoyable and interesting sojourn.

[28] D. A. Bromley and E. Almqvist, *Reports on Progress in Physics* (The Physical Society, London, 1959), Vol. 23, p. 544.

PHYSICAL REVIEW VOLUME 124, NUMBER 5 DECEMBER 1, 1961

Excitation Functions of $K^{41}+p$ Reactions*

R. D. SHARP, L. F. CHASE, JR., R. M. FRIEDMAN,† E. K. WARBURTON,‡ AND E. G. SHELLEY
Research Laboratory, Lockheed Missiles and Space Company, Sunnyvale, California

(Received July 12, 1961)

The energy of some of the gamma radiation following the proton bombardment of K^{41} has been measured, and the origins of some of these gamma rays have been determined. The excitation functions of the 1.00-Mev gamma from inelastic scattering in K^{41} and the 2.16-Mev gamma from the $K^{41}(p,\alpha\gamma)$ reaction have been measured in a region between 2.3 and 3.5 Mev and approximately 50 resonances observed. The energies and absolute cross sections, and the anisotropy of the gamma radiation proceeding from some of these resonances have been measured, leading to information on the excited states in Ca^{42} at about 13-Mev excitation, including an upper limit on the average level spacing. Evidence is given to show the 100-Mev level in K^{41} is most likely a $\frac{1}{2}+$ state in agreement with theoretical predictions.

INTRODUCTION

THE low-lying states of nuclei near the doubly magic Ca^{40} are of particular interest from the point of view of the jj-coupling shell model. Recent theoretical analyses have yielded results in good agreement with experiment,[1–3] while other specific predic-

* Supported by the joint program of the U. S. Atomic Energy Commission and the Lockheed General Research Program.

† Now at Aerospace Corporation, El Segundo, California.

‡ Permanent Address: Physics Department, Princeton University, Princeton, New Jersey.

[1] C. Levinson and K. W. Ford, Phys. Rev. **99**, 792 (1955); **100**, 11 (1955).

[2] J. B. French and B. J. Raz, Phys. Rev. **104**, 1411 (1956).

[3] S. P. Pandya, Progr. Theoret. Phys. (Kyoto) **19**, 404 (1958).